Geoderma 433 (2023) 116447

Contents lists available at ScienceDirect

Geoderma

journal homepage: www.elsevier.com/locate/geoderma

Soil salinity determines the assembly of endophytic bacterial communities in the roots but not leaves of halophytes in a river delta ecosystem

Yi Zhou [a,b], Yanli Wei [b], Maarten Ryder [a,b], Hongmei Li [b], Zhongjuan Zhao [b], Ruey Toh [a], Peizhi Yang [c], Jishun Li [b], Hetong Yang [b], Matthew D Denton [a,b,*]

[a] School of Agriculture, Food and Wine, The University of Adelaide, Urrbrae, SA 5064, Australia
[b] China-Australia Joint Laboratory for Soil Ecological Health and Remediation, Ecology Institute, Qilu University of Technology (Shandong Academy of Sciences), Shandong 250013, China
[c] College of Grassland Agriculture, Northwest A&F University, Yangling, Shaanxi 712100, China

ARTICLE INFO

Handling Editor: Matthew Tighe

Keywords:
Bacteria
Endosphere
Phyllosphere
Beneficial microbe
Plant-growth promoting bacteria

ABSTRACT

Although soil and rhizosphere microbiomes in highly saline environments have been well-studied, the role of soil salinity in the ecological processes affecting endophyte colonization and persistence remain largely unclear in halophytic plants. The present study sampled young and mature plants of the halophyte *Suaeda salsa* from 42 sites in the Yellow River Delta, China that varied in soil salinity. Soil physicochemical properties, root and leaf microbiomes, phylogenetic variation among plant ecotypes, and leaf metabolites were analysed. In the roots of both young and mature plants, soil salinity significantly influenced the composition of the endophytic microbiota ($r = 0.29 \sim 0.45$, $P < 0.001$), and negatively correlated with endophyte alpha-diversity ($r = -0.75 \sim -0.78$, $P < 0.001$). Leaf microbiome dissimilarity increased with geographic distance ($r = 0.17 \sim 0.26$, $P < 0.001$), based on a distance-decay model, and was associated with plant phylogenetic variation ($r = 0.15$, $P = 0.015$ for young plants only). Additionally, leaf microbiome diversity and composition were correlated with soil age, pH, P content, and certain leaf metabolite compounds, but not with soil salinity. The dominant genera observed in young roots were *Mesorhizobium* spp. and *Rhodomicrobium* spp., while *Pelagibius* spp. was dominant in mature roots, and *Pseudomonas* spp. and *Kushneria* spp. were dominant in leaves. Soil salinity exerted a strong deterministic effect on the diversity and composition of the root endophyte community, while the acquisition and assembly of the leaf microbiome was affected by the dispersal effects, and the leaf metabolism of the host halophyte.

1. Introduction

Soil salinity affects over 6% of global terrestrial ecosystems (Munns, 2005), and can form an extreme environment that comprises unique microbe-plant-soil relationships (Vimal et al., 2017). As the reservoir for the microbes colonizing the plant root, and even the stems and leaves, the soil bacterial community is structured by salinity to a greater extent than by other physicochemical factors such as temperature and pH, based on a survey of over 100 globally distributed natural environments (Lozupone and Knight, 2007). Halophytes, plants that are able to grow in saline soils, have developed mechanisms to enable survival under saline conditions, including the exclusion of salts from organs, osmotic adjustment, and the isolation and storage of ions in specific organs (Hardoim et al., 2015). These mechanisms provide a different microhabitat for microbes to colonize compared with non-halophytes. Additionally, the association with microorganisms, such as bacteria, can promote plant growth and adaptation to salinity (Kearl et al., 2019). Therefore, halophyte-associated microbiomes and their assemblage mechanisms under saline environmental conditions differ from plant microbiomes found in benign habitats that are better understood.

Halophyte endophytic communities are characterised by halotolerant bacteria with plant growth promoting capabilities in other plant

Abbreviations: YRD, Yellow River Delta; ASV, amplicon sequence variant; KEGG, Kyoto Encyclopedia of Genes and Genomes; MSTFA, N-methyl-N-trimethylsilyltrifluoroacetamide; ML, maximum likelihood; NMDS, nonmetric multidimensional scaling; PERMANOVA, permutational multivariate analyses of variance; AIC, Akaike Information Criteria; STAMP, Statistical Analysis of Metagenomic Profiles; MaAsLin2, Multivariate Association with Linear Models 2.

* Corresponding author.
E-mail address: matthew.denton@adelaide.edu.au (M.D. Denton).

https://doi.org/10.1016/j.geoderma.2023.116447
Received 26 July 2022; Received in revised form 2 February 2023; Accepted 22 March 2023
Available online 31 March 2023

species (Li et al., 2021). For example, *Halomonas* spp., *Bacillus* spp., and *Kushneria* spp. were consistently isolated from the roots of three native Utah halophytes and were able to improve the growth of alfalfa crops in saline conditions (Kearl et al., 2019). Additionally, a *Pseudomonas* spp. strain isolated from the *Suaeda salsa* rhizosphere was able to reduce salinity stress in rice seedlings (Yuan et al., 2016). Halotolerant bacteria can improve plant salt tolerance through osmolyte accumulation, regulation of ion homeostasis, improved nutrient uptake, regulation of plant hormone production, and induction of antioxidant-based defence systems (Saghafi et al., 2019). A range of microbial species were identified as halotolerant endophytes, and their diversity was associated with the halophytic plant species and the growing environment, which suggests that microbe-host-environment specific interactions can operate under saline conditions (Kearl et al., 2019).

Recently, plant microbiota, including their community structure and diversity in above- and belowground plant anatomical compartments, have been investigated in model species (Bai et al., 2015; Bulgarelli et al., 2012) and in economically important species (Cernava et al., 2019; Grady et al., 2019; Sun et al., 2021; Zarraonaindia et al., 2015). The assemblage of root microbiome was driven by the recruitment process of host plant (Muller et al., 2016; Zhou et al., 2020), and extreme environments may modulate the metabolism and growth of the host plant and its selective effect on root-associated microbiota. For example, host phylogeny was associated with root endophyte composition among grass species (Naylor et al., 2017), while the correlation was weakened by drought stress. Additionally, in the extreme environment of the Namib Desert, root-associated microbial communities of different speargrass species were not correlated with their phylogenetic turnover (Marasco et al., 2018). Previous studies have also demonstrated that salinity history and salinity concentration considerably altered the assembly of root microbiomes in halophytes (Furtado et al., 2019; Mukhtar et al., 2021; Rath et al., 2019; Szymanska et al., 2018; Zhao et al., 2022). However, each of these studies was performed in only two to three saline environments, which was not adequate to identify the complexity of various environmental factors shaping endophyte communities of the halophyte root.

The structure and diversity of the microbial community in the plant leaf was influenced by environmental changes (e.g., fertilizer application) to a lesser extent than the soil microbiome (Sun et al., 2021). Leaf microbiome structure was highly associated with host evolutionary relatedness among 57 neotropical forest tree species (Kembel et al., 2014). In contrast, in a further study leaf microbial taxa were conserved among three unrelated meadow plant species (Massoni et al., 2020). Additionally, in some plant species, diverse metabolites accumulate in leaves, and may exert a strong selection pressure on leaf microbiome colonisation, e.g., the bioactive metabolites produced by *Arugula* leaves were related to the enrichment of various members of the *Enterobacteriaceae* spp. characterised with antibiotic resistance compared with belowground organs (Cernava et al., 2019). The leaves of *S. salsa* are high in soluble sugars, organic acids and amino acids (Li and Song, 2019), and their concentrations are sensitive to soil salinity concentrations (Zang et al., 2021). Therefore, soil salinity might shape the microbiome by modulating metabolites in *S. salsa* leaves, although the detailed processes have not been well studied.

The present study focused on the microbiome of *S. salsa*, a euhalophyte native to the Yellow River Delta (YRD), China. The YRD is characterized by extreme environments as a result of salt water encroachment, and soil salinity patterns that vary independently of geographic location. Here, we sampled 42 populations of *S. salsa* from locations covering a large proportion of the YRD, with diverse soil characteristics, particularly salinity concentrations. The objectives were to evaluate the effects of soil properties, geographic location, plant genetic variation, leaf metabolism and plant development on the assemblage of endophytic communities, and to determine the core root- and leaf-associated microbiomes of this halophyte across different geographic sites.

2. Materials and methods

2.1. Sample collection, processing and storage

Samples for the present study were collected in the Yellow River Delta (YRD). The Yellow River carries the highest sediment load in the world, and the region is characterized by extensive soil salinization, with high and variable severity, due to patterns of fresh water discharge from the Yellow River and seawater intrusion (Guan et al., 2019). *Suaeda salsa* (Amaranthaceae) is a pioneer species and the dominant native halophyte in saline soil in the YRD, even occurring along the coastal region of the YRD. Habitats with diverse soil salinity in the YRD provide an opportunity to study the plant genetic diversity and associated microbiome diversity of *S. salsa* plants.

In October 2018, *S. salsa* plants were collected from 42 sites in the YRD including three different ages of soils based on the historical changes of coast lines (Fig. S1). At each site, a plot (10 m × 10 m) was marked, and 10 young plants (8–10 cm shoot length, and no inflorescence observed), 10 mature plants (15–20 cm shoot length with inflorescence in every leaf axil), and 10 bulk soil samples were collected, including all the leaves, roots to 10 cm depth, and bulk soil next to the plant (10 cm diameter × 10 cm depth). The 10 subsamples were mixed into one sample per site for young leaf, young root, mature leaf, mature root and bulk soil, respectively. Totally, 210 samples were collected in the field, and then transported to the lab at 4 °C in a portable car fridge.

Plant tissue samples were processed to remove surface-attached microbes (in the rhizosphere and phyllosphere) using a method modified from that of Bulgarelli et al. (2012). The sampled plant tissues were transferred into 50 ml Falcon tubes with 30 ml sterile phosphate-buffered saline (about 10 g sample per tube), and then placed on an orbital shaker for 20 min at 180 rpm. Roots or leaves were picked up using sterilised tweezers, transferred into new Falcon tubes, and the procedure was repeated. Finally, the Falcon tubes containing plant tissues were sonicated for 10 cycles of 30 s at 43 kHz and 120 W power (model 160HD, Soniclean, Australia) with 30 s breaks. The washed root and leaf samples were stored at −80 °C for the DNA extraction and metabolite analysis. For the bulk soil samples, 10 g were stored at −80 °C for the DNA extraction. The rest was air-dried, and then stored at 4 °C for analysing physical and chemical properties.

2.2. Microbiome analysis

Leaf and root tissues were ground in liquid nitrogen and subsampled (0.5 g) to extract DNA using the PowerSoil DNA isolation kit (MoBio Labroratories, Carlsbad, CA, USA) according to the manufacturer's instructions. Soil DNA extraction was conducted using the same kit from 0.5 g bulk soil per sample.

The V3-V4 region of the bacterial 16S rRNA gene was amplified using the primers 341F (5′- CCTACGGGNGGCWGCAG −3′) and 805R (5′- GACTACHVGGGTATCTAATCC −3′) (Thijs et al., 2017). PCR products were sequenced on the Illumina Miseq™ platform with 300 bp length of PE reads. All of the sequence data generated in the present study have been uploaded on National Center for Biotechnology Information with the project ID: PRJNA853873. Quantitative Insights Into Microbial Ecology 2 (QIIME2, vs. 2017.6.0) software was used to analyse the sequences of 16S rRNA genes (Bolyen et al., 2019). Raw reads were processed, including demultiplex by "q2-demux" in QIIME2, and quality control was assessed with "q2-cutadapt". The DADA2 denoising option (Callahan et al., 2016) was selected to pick up the representative reads for generating an amplicon sequence variants (ASVs) table. ASVs were assigned using the SILVA reference database vs. 132 (Quast et al., 2013). The ASV table with taxonomic data was used to predict the functional profiles of the microbial community by *Tax4Fun* package in R (Aßhauer et al., 2015). Microbial functions were annotated using the Kyoto Encyclopedia of Genes and Genomes (KEGG) database, release 85.0, 2018 (Kanehisa and Goto, 2000). Relative abundance of level-2

functional groups were compared between niches.

2.3. Leaf metabolite analysis

Leaf metabolite analysis was done according to a protocol modified from Cohen et al. (2016) and Lu et al. (2019). Firstly, all the cleaned leaves were processed by freeze-drying for 24 h, grinding in liquid nitrogen, and subsampling approximately 5 g for ultra-grinding (20 Hz for 5 min, model MM400, Retsch, Germany). Finally, 20 mg powder was transferred into 2 ml tubes with 1 ml of 4 °C pre-cooled extraction buffer (2.5:1:1 mixture by volume of HPLC-grade methanol, HPLC-grade chloroform and HPLC grade water) containing a DL-norleucine internal standard. The tubes were vortexed for 2 min, and centrifuged at 10,000 g for 10 min at 4 °C. The supernatant was collected into fresh 2 ml tubes and 300 μl of HPLC-grade chloroform and 300 μl of HPLC-grade water were added. The tubes were vortexed for 2 min and centrifuged at 10,000 g for 10 min at 4 °C, and then 300 μl aliquots from the supernatant were transferred into a glass vial for vacuum-drying at room temperature.

The dried aliquots were derivatized by (1) adding 40 μl of methoxyamine hydrochloride solution into the vial, vortexing for 30 s and reacting for 2 h at 37 °C, and then (2) adding 70 μl of N-methyl-N-trimethylsilyltrifluoroacetamide (MSTFA) containing pre-mixed *n*-alkanes, and reacting for 1 h at 70 °C. Finally, derived samples were cooled to room temperature.

Analyses were performed on a Gas chromatography–mass spectrometry (GC–MS) system (model 7890A, Agilent Technologies, Santa Clara, CA, USA) equipped with a mass selective detector (model 5975c, Agilent Technologies, Santa Clara, CA, USA) and a DB-5 capillary column (30 m × 0.25 mm × 0.25 μm, Agilent J&W Scientific, Folsom, CA, USA). Firstly, 1 μl of the derivatized sample was injected into the GC column using splitless mode, helium gas with a flow rate of 1 ml min^{-1}, and injection temperature of 260 °C. Then, mass spectra were collected using a 70 eV electron beam, 30–600 m z^{-1} scanning range, and 20 spectrum s^{-1} recording rate. One pooled sample was prepared as the quality control.

The raw data from the GC–MS system was processed using Mass Hunter software (version B.07.01, Agilent Technologies, Santa Clara, CA, USA). Peak area integration was calculated and normalized across different samples using the DL-norleucine internal standard signal. Annotation was performed based on the public database MassBank version 2020.10 (Horai et al., 2010) and KNApSAcK metabolite-species database, version 1.200.03 (Afendi et al., 2012) with a 70% similarity cut-off (Wang et al., 2015).

2.4. Plant phylogenetic and soil physicochemical analysis

Different leaves from one mature plant per site were used to extract plant DNA using the CTAB method (Doyle and Doyle, 1990). A non-coding region of chloroplast DNA, *rpl32-trn*L was amplified using PCR (primer F: 5′- CAGTTCCAAAAAAACGTACTTC −3′; R: 5′-CTGCTTCCTAAGAGCAGCGT-3′ Shaw et al., 2007, with initial denaturation at 95 °C for 5 min, 30 amplification cycles comprising 95 °C for 1 min, 52 °C for 1 min, and 72 °C for 1 min, final extension at 72 °C for 7 min). Previous studies have demonstrated the effectiveness of *rpl32-trn*L to identify the phylogenetic structure of *Suaeda* species (Park et al., 2019; Shaw et al., 2007). The PCR product was sequenced on the ABI 3730 XL platform (Applied Biosystems, Foster City, CA). Bidirectional sequences were assembled, aligned by MAFFT version 7 (Katoh et al., 2017), and trimmed using Gblocks 0.91b (Castresana, 2000). Maximum likelihood (ML) analyses were performed using raxmlGUI version 1.5b2 (Silvestro and Michalak, 2012) by selecting ML + bootstrap option using 500 replicates. Finally, phylogenetic distance between samples was generated.

Soil physical and chemical properties including electrical conductivity (EC), pH, organic carbon, total N, total P, total K, and texture were analysed according to the protocol of Rayment and Lyons (2011) using the bulk soils collected at each site.

2.5. Statistical analysis

Firstly, ASVs annotated as “Chloroplast” or “Mitochondria” were removed from the analysis, as they were regarded as plant organellar ASVs. Low frequency ASVs were also removed if there were<5 counts across all the samples in the experiment. The filtered ASVs table was normalized using the trimmed mean of M values method from the Bio-Conductor *EdgeR* package version 2.9 in R version 3.3.3 (R Core Team, 2013).

Nonmetric multidimensional scaling (NMDS) analysis was conducted, and Bray-Curtis distances among paired samples were estimated using the *Vegan* package version 2.4–5 (Oksanen et al., 2007). The effects of plant age (young and mature), organ (leaf and root) and their interactions on microbial ASV composition were tested by permutational multivariate analyses of variance (PERMANOVA) using Bray-Curtis distance (*adonis* function in the *Vegan* package). Analysis of similarity (ANOSIM) based on the Bray-Curtis distance was used to elucidate whether the microbial community structure was significantly different between niches (*anosim* function in the *Vegan* package).

The distance matrices among the 42 samples for soil characteristics (Euclidean distance), leaf metabolites (Euclidean distance), and geography (geographic distance) were calculated, using Mantel analysis and partial Mantel analysis, based on Pearson correlation with 999 permutations, to test the association between distance matrices of microbiome composition, soil properties, metabolite composition, geography, and plant phylogenetic variation, using the *Vegan* package.

A distance-decay model was used to test the relationship between microbiome similarity and geographic distance. The model is $\log_{10}(S) = (-2z)*\log_{10}(d) + b$, where S is the community similarity matrix calculated as 1-Bray-Curtis distance, d is the geographic distance (m) matrix between samples, and z is the turnover rate (Zhou et al., 2022). The model fitness was tested for the microbiome in the leaf and root of young and mature plants, and bulk soil, respectively.

The effects of different vectors indicating soil properties and plant metabolism on microbiome composition were analysed by building up multivariate models. Adding or removing a regressor was decided based on the minimum values of the Akaike Information Criteria (AIC) using the *step* function in the *Vegan* package in R. PERMANOVA was performed based on the AIC-selected model using the *adonis* function. Meanwhile, multiple regression analysis was conducted to test if Shannon index was correlated with the factors of soil property and plant metabolism. A stepwise selection from both “forward” and “backward” with AIC minimization was used from the *stepAIC* function in *Vegan* package. Normal distribution was tested prior to multivariate analyses, and $\log_{10}$-transformation was applied to the variables that were not normally distributed.

The core microbiomes present in each of the plant organs at both plant ages across the sampled sites were established. Firstly, only the highly abundant and ubiquitous ASVs were kept, using two criteria: (a) the top 10% mean relative abundance of all samples and (b) those present in > 80% of all samples (Delgado-Baquerizo et al., 2018; Jiao et al., 2019). The selected ASVs were defined as coreASVs for each niche. In addition, the unique ASVs (the ASV present in one site and absent in the others) were also identified in each site for young and mature root and leaf, respectively.

We examined the effects of plant age (young and mature), organ (leaf and root), soil factors and leaf metabolites on the relative abundance of microbial genera and functional categories. Firstly, an ANOVA test for the effect of age and organ on relative abundance of each microbial genus and functional group was performed using the Statistical Analysis of Metagenomic Profiles (STAMP) package version 2.1.3 (Parks et al., 2014). A Benjamini-Hochberg False Discovery Rate (FDR) test was applied in STAMP to adjust P values. In addition, Multivariate

Association with Linear Models 2 (*MaAsLin2*) package version 2.0 in R (Mallick et al., 2021) was used to correlate the relative abundance of microbial genera and functions with the environmental and metabolic factors. The correlation coefficient (r) and the adjusted P value using the Benjamini-Hochberg FDR method were calculated.

3. Results

3.1. Microbiome diversity of Suaeda salsa roots and leaves at different developmental stages

In total, microbiomes of 210 samples were analysed, including bulk soil, and *S. salsa* plant roots (young and mature) and leaves (young and mature) from 42 sites. The sequence depth of all the samples was 170,806–265,840 (201,182 on average) PE reads with 300 bp length, and the number of clean reads after quality control was 154,404 to 256,443 with average of 192,726 in 210 samples. Firstly, nonmetric multidimensional scaling (NMDS) analysis was performed to evaluate the differentiation of ASV composition between samples (beta-diversity). This revealed a clear separation between bulk soil, root and leaf samples (Fig. 1a). The overlap between mature and young plants was larger in the roots than in the leaves, based on 95% confidence to cover all the samples in each niche (Fig. 1a). Further statistical testing of microbial ASV composition by permutational multivariate analysis of variance (PERMANOVA) also showed a significant plant organ × plant age interaction ($P < 0.01$, Table 1). In addition, analysis of similarity (ANOSIM) test also indicated the significant effect of plant age and organ on the microbial community structure ($P < 0.01$), and r value for the plant age effect was higher than organ (0.869 vs 0.124, Table 1).

The Shannon index, that was calculated to indicate the alpha-diversity of microbial communities, was lower in plant organs than in bulk soil (4.1 vs 7.9, $P < 0.05$, Fig. 1b). No organ × plant age interaction in Shannon index was detected ($P > 0.05$, Table 1), and the Shannon index of the root microbiome was higher than in the leaf, and was higher for older plants than for young plants (Fig. 1b).

3.2. Geographic effect, soil history, edaphic factors, and plant leaf metabolites related to microbiome composition in S. Salsa roots and leaves at different developmental stages

The geographic effect was tested using the distance-decay model. For leaf endophytes in both young and mature plants, the similarity of microbiome composition declined significantly with increased geographic distance ($P < 0.01$, Fig. 2a), while no distance-decay pattern was observed for the microbiomes in roots or bulk soil.

The influence of soil age, edaphic factors and plant metabolites in shaping the composition of microbiome at different plant niches was evaluated further by multiple stepwise regression analysis (Table 2). Soil age was the key factor associated with microbiota structure in bulk soil. Soil salinity (EC) contributed significantly to the root microbiota assembly in both young and mature plants ($P < 0.01$, Table 2). Microbial composition was correlated with soil age, pH and P content for mature leaves, and soil age and pH for young leaves. Likewise, there was a significant association between the increased dissimilarity of microbiota composition and the enlarged difference in soil EC for the root microbiome, but not for the microbiomes in leaf and bulk soil (Fig. 2b). Samples of bulk soil were separated by soil ages in the biplot of NMDS analysis (Fig. S2). Among the leaf metabolites, tyrosine and gluconic lactone were found to associate with microbiome structure in mature leaves and young leaves, respectively ($P < 0.01$, Table 2).

Dissimilarity matrices were generated using all the measured traits including geographic distance, soil properties, leaf metabolites, plant phylogenetic variability, and plant microbiome composition, and a correlation analysis (Mantel analysis) was run between the matrices. Microbiome composition was highly correlated between the young and mature plants in roots or leaves ($P < 0.05$, $r = 0.50–0.81$, Fig. S3). Significant correlations of geographic distance vs plant phylogenetic distance were observed, and when geographic distance was controlled, partial Mantel analysis showed that there was no correlation between plant phylogenetic distance and microbiome (Fig. S3). Leaf metabolite composition was not associated with leaf microbiome structure, and edaphic distance were not associated with bulk soil microbiome composition.

3.3. Soil history, edaphic factors and plant leaf metabolites related to alpha diversity of S. Salsa root and leaf microbiomes at different developmental stages

Microbiome alpha diversity was indicated by the Shannon index, and multiple regression analysis showed that among all the measured soil traits, only soil EC was associated with alpha diversity of the root microbiomes for both young and mature roots ($P < 0.05$, Table 3). Pearson correlation was performed to analyse the relationship between soil EC and the alpha diversity of root microbiota, and a negative regression relationship was detected (Fig. 3a and b). Alpha diversity of the bulk soil microbiome significantly responded to soil age ($P < 0.05$, Table 3), and the microbial community was less diverse in the youngest soil (<90 yr) than in the older soils (90–170 yr and > 170 yr, Fig. S2).

In addition, soil age and pH were identified as significant predictors of alpha diversity for mature leaf microbiomes from multiple regression analysis of all the soil traits, and microbiome alpha diversity in young leaves was significantly affected by soil age and P content (Table 3). Individual regression analysis confirmed the significant negative relationship between soil pH and alpha diversity of mature leaf microbiomes, and the positive correlation between soil P content and alpha diversity for young leaf microbiomes (Fig. 3 c and d).

Five and fifteen metabolites were associated with microbiome alpha diversity in mature and young leaves, respectively (Table 3). Three metabolites, tartaric acid, citric acid and methionine, were correlated with the microbial diversity of both young and mature leaves. In mature leaves, 2-hydroxypyridine had the highest t-value to correlate with alpha diversity (Table 3).

3.4. The core and unique microbes in S. Salsa roots and leaves at different developmental stages

The number of coreASVs in bulk soil was the largest (552, Fig. 4a), and the number decreased from root (23 to 70) to leaf (7 to 11). At least threefold more coreASVs were found in mature roots than in young roots, while the difference between young and mature leaves was less, at 11 vs 7 (Fig. 4a). Most of the bulk soil coreASVs (about 90%) were not detected among plant coreASVs. There was a number of coreASVs shared between mature and young plants. Out of 70 coreASVs in mature roots, only 33 (about 47%) were found in bulk soil.

Annotation of coreASVs showed that at the phylum level, the number of coreASVs belonging to Proteobacteria was larger than those of other phyla in all of the soil and plant niches (Fig. 4b). The proportion of Proteobacteria coreASVs increased from the soil microbiome to inner endophytes communities, and was higher in the mature tissue than the young tissue. At the genus level, there was a large number of young plant coreASVs belonging to *Mesorhizobium* spp. and *Rhodomicrobium* spp., e.g., > 25% of the total coreASVs number for young roots and > 50% for young leaves (Fig. S4). *Pseudomonas* spp., *Kushneria* spp., *Pantoea* spp. and *Cryobacterium* spp. accounted for a major proportion of coreASVs (36%-57%) in the leaf microbiome, but were minor in root and bulk soil microbial communities.

The richness of unique ASVs relative to the total ASVs was greater in the young tissues than the mature tissues (Fig. S5a). The unique ASVs richness in mature leaf was negatively correlated with soil P and K content (Fig. S5b), and no other significant correlation was observed between the richness of unique ASVs and soil properties in different endophytic niches.

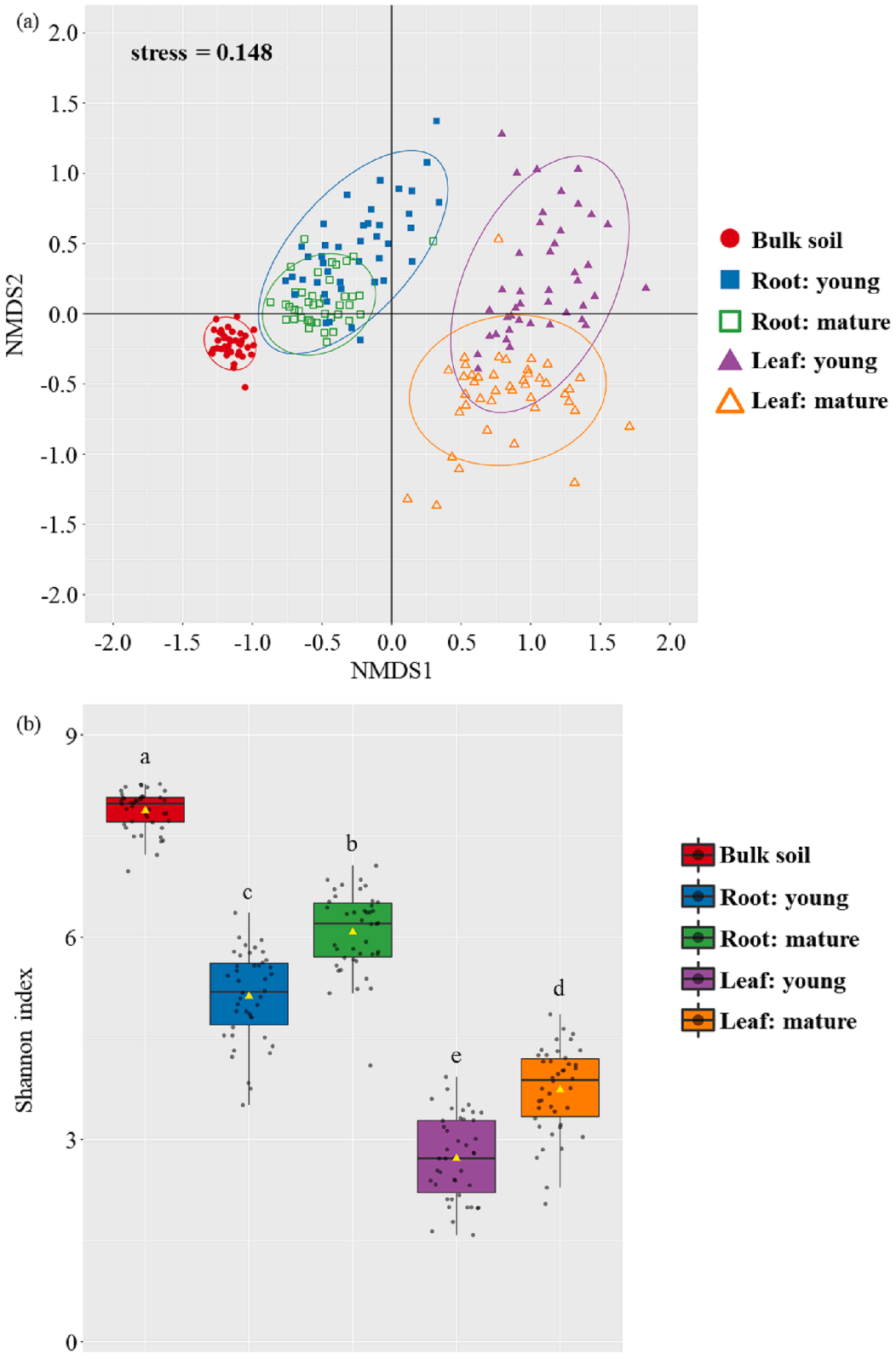

Fig. 1. Composition and alpha diversity of microbial communities in plant-soil niches of *Suaeda salsa* Plant niches include roots and leaves of young and mature *Suaeda salsa* plants sampled from 42 sites in the Yellow River Delta, China. (a) Biplot based on nonmetric multidimensional scaling (NMDS) analysis, ellipses indicate 95% confidence level to cover all the samples in each niche. (b) Shannon index of microbiomes. The values for individual samples are presented in the boxplot, the yellow triangle is the mean, and the box and central line represent first quartiles, medians, and third quartiles, respectively. The distribution of data points along horizontal axis within each box is randomized. The same letters indicate no significant differences ($P < 0.05$) between niches based on Tukey HSD post-hoc pairwise comparison testing.

Table 1
The effect of plant organ (root and leaf) and plant age (young and mature) on microbiome diversity of *Suaeda salsa*. Plants were collected from 42 sites (n = 42). Microbiome diversity includes beta-diversity described by Bray-Curtis distance and alpha-diversity indicated by Shannon index. Permutational multivariate analyses of variance (PERMANOVA) and Analysis of similarities (ANOSIM) were performed to analyse Bray-Curtis distance.

	PERMANOVA Degrees of Freedom	Sum of Squares	F-value	R^2	*P*-value	ANOSIM r	*P*-value	Shannon index *P*-value
Organ	1	11.51	36.37	0.17	< 0.01	0.869	< 0.01	< 0.01
Plant age	1	2.522	7.969	0.037	< 0.01	0.124	< 0.01	< 0.01
Organ × plant age	1	1.844	5.827	0.027	< 0.01			0.727

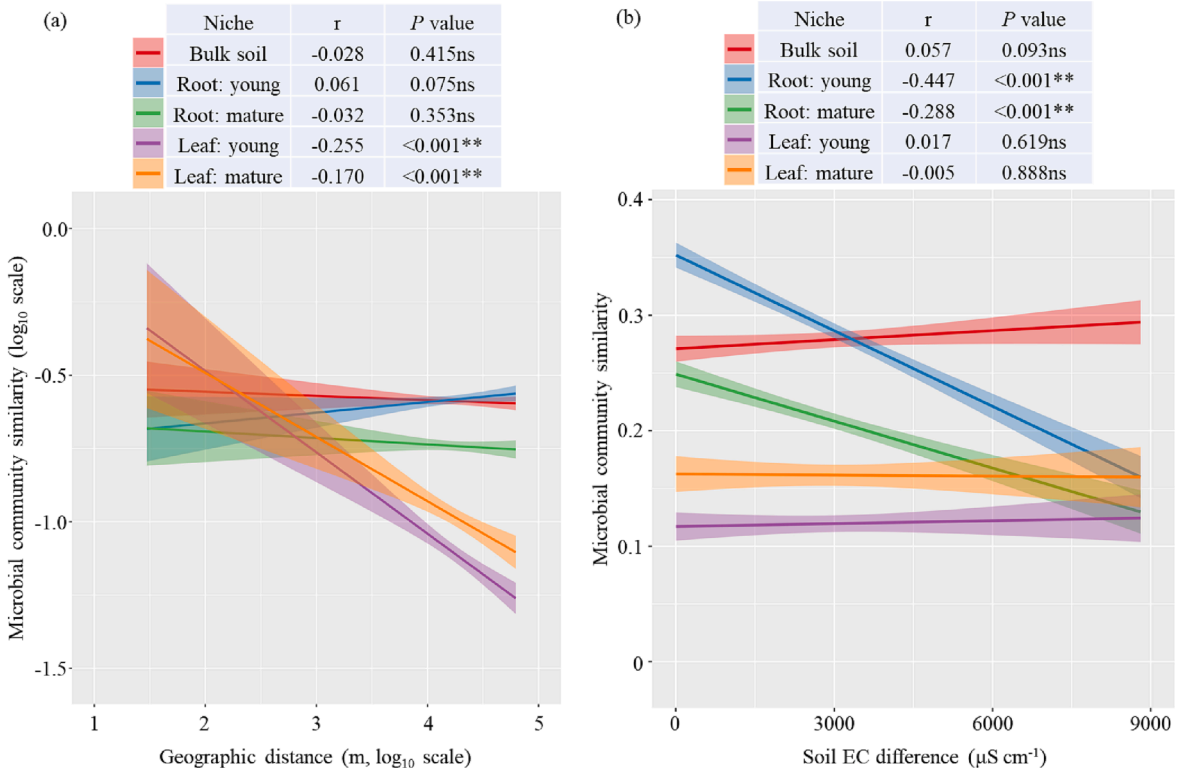

Fig. 2. The effects of (a) geographic distance and (b) soil salinity on microbial community composition in plant-soil niches of *Suaeda salsa* Plant niches include roots and leaves of young and mature *Suaeda salsa* plants sampled from 42 sites in the Yellow River Delta, China. Microbiome similarity between samples was calculated using (1 - Bray-Curtis distance). A distance-decay model was used to test the relationship between microbial community similarity and geographic distance. The r values are presented, and ns, * and ** indicate not significant, and significant at P < 0.05 and P < 0.01 for the correlation, respectively.

3.5. The dominant microbes in S. Salsa roots and leaves at different developmental stages

In each niche of plant organ and plant age, the dominant genera were defined as having > 3% average relative abundance and being present in > 80% of all samples. The relative abundance of dominant genera was compared between different niches across the 42 sampling sites (n = 42). The relative abundance of *Mesorhizobium* spp. and *Rhodomicrobium* spp. in young roots was 14.6% and 26.8%, respectively, which was significantly higher (adjusted P < 0.01) than in other microhabitats (0.14% − 5.1%, Fig. 4c). The mature roots harboured more *Pelagibius* spp. than other niches (5.5% vs 0.32%-2.1%, adjusted P < 0.01). *Pseudomonas* spp. and *Kushneria* spp. were more abundant in leaf microbiomes than in other niches. Young and mature leaves had similar relative abundances of *Pseudomonas* spp., but more *Kushneria* spp. were detected in mature leaves than in young leaves (12% vs 7.4%).

Associations between the abundance of microbial genera and soil–plant factors (soil properties and leaf metabolites) were analysed, and a significant correlation (adjusted P < 0.05) was found only for *Kushneria* spp. in the mature leaf microbiome. The increased relative abundance of *Kushneria* spp. in the mature leaf was related to increased leaf metabolite concentrations of fructose, D-arabitol, oxoproline, ornithine, proline, 3,4-dihydroxybenzoic acid, benzoic acid and naringenin (adjusted P < 0.01, Fig. S6).

3.6. The predicted functions of microbiomes in S. Salsa roots and leaves at different developmental stages

The analysis of microbial potential functions showed that leaf microbiomes had a higher relative abundance of carbohydrate metabolism, especially for the mature plants, and lower relative abundance of energy metabolism, metabolism of cofactors and vitamins, and lipid metabolism than soil and root (adjusted P < 0.05, Fig. S7). The metabolism of amino acids was highly enriched in bulk soil compared with the plant niches. For microbial functions related to processing of environmental information, membrane transport was more abundant in the root microbiome, especially in the mature plant, than in other niches, while the proportion of signal transduction activities was greater in the leaf microbiome. Young roots were colonised by microbes with more active functions in genetic information processing. The microbiome function of cell motility decreased along the sequence from bulk soil to root to leaf.

Table 2
The effects of soil property and plant metabolism on microbiome composition in *Suaeda salsa* plant-soil niches. A multiple stepwise regression model was used to select the vectors of soil traits and metabolites based on the minimum values of the Akaike Information Criteria (AIC), and test the significance of model fitness. Only the significant correlations ($P < 0.05$) were presented. The selected factors were analysed by permutational multivariate analyses of variance (PERMANOVA). *: significant at $P < 0.05$, and **: significant at $P < 0.01$.

Niche of microbiome	Explanatory factors	Multiple stepwise regression model		PERMANOVA test
		Model fitness	Significant factors	(R^2 value)
Bulk soil	Soil traits	AIC = 99.8	Soil age	0.076**
Mature root	Soil traits	AIC = 105.6	EC	0.065**
Young root	Soil traits	AIC = 90.61	EC	0.063**
Mature leaf	Soil traits	AIC = 108.8	Soil age	0.058**
			Soil P content	0.057**
			pH	0.049*
Young leaf	Soil traits	AIC = 115.3	Soil age	0.057**
			pH	0.027*
Mature leaf	Metabolites (mature leaf)	AIC = 109.2	Tyrosine (Amino acids)	0.051*
Young leaf	Metabolites (young leaf)	AIC = 112.3	Gluconic lactone (Carboxylate)	0.041*

The effect of soil salinity on the relative abundance of functional groups in the various microbiomes was tested for every niche (Fig. 5). Highly significant correlations with soil salinity ($r > 0.05$ and adjusted P < 0.01) were found for energy metabolism activities in bulk soil, metabolism of cofactors and vitamins in young root, and membrane transport in mature roots. Furthermore, functional groups of root endophytes actives were more sensitive to changes in soil salinity, compared with bulk soil and leaf (especially mature leaf) microbiomes.

4. Discussion

Our study investigated the endophytic bacterial communities of leaf and root in young and mature plants of the halophyte *S. salsa* across 42 saline environments in the Yellow River Delta. Salinity is considered to be a key driver structuring microbial consortia based on a global soils (Lozupone and Knight, 2007), and aquatic ecosystems (Herlemann et al., 2011). Microbial communities in saline soil and in the rhizosphere soil of halophytes have been explored at larger geographic scales to elucidate the effect of environmental factors on the development of microbiome structure and diversity (Guan et al., 2021; Liu et al., 2020a; Liu et al., 2020b). However, the ecological processes that shape endophytic colonization by microbes and their persistence in halophytic plants remain largely unexplored and unresolved. Our results reveal that soil salinity exerts a strong deterministic effect on the diversity and composition of root endophytic communities, while the acquisition and assembly of leaf microbiomes was influenced by the dispersal effect, such as soil age and geographic distance, and the metabolism of the host halophyte.

4.1. Microbiome assemblages differed between leaves and roots, and between developmental stages of S. Salsa

In the present study, plant organ (leaf compared with root) played a greater role in determining microbiome structure than developmental stage. Roots and leaves are different ecological microhabitats, and are

Table 3
Alpha-diversity of microbiome in *Suaeda salsa* plant-soil niches influenced by soil property and plant metabolism. Shannon index was used to indicate alpha-diversity. Multiple regression analysis was conducted to test the correlation between Shannon index and the factors of soil property and plant metabolism. A stepwise selection was used based on the minimum values of the Akaike Information Criteria (AIC) and the significance of model fitness. Only the significant correlations ($P < 0.05$) were presented. *: significant at $P < 0.05$, and **: significant at $P < 0.01$.

Niche of microbiome	Model fitness Explanatory factors	AIC	R^2	p-value	Significant factors	t value
Bulk soil	Soil traits	−112.1	0.310	<0.01	Soil age	4.16**
Mature root	Soil traits	−78.29	0.625	<0.01	EC	−7.20**
Young root	Soil traits	−74.30	0.656	<0.01	EC	−8.61**
Mature leaf	Soil traits	−43.53	0.257	<0.01	Soil age	2.17*
					pH	−2.97**
Young leaf	Soil traits	−47.05	0.276	<0.01	Soil age	2.06**
					Soil P content	−2.39*
Mature leaf	Metabolites (mature leaf)	−85.28	0.532	0.032	Threitol (Alcohols)	−3.42*
					Aspartic acid (Amino acids)	−3.24*
					Tartaric acid (Carboxylate)	3.09*
					Citric acid (Carboxylate)	2.97*
					Methionine (Amino acids)	2.71*
Young leaf	Metabolites (young leaf)	−221.1	0.958	0.039	2-hydroxypyridine (Others)	12.6*
					Tyrosine (Amino acids)	−7.82*
					Tartaric acid (Carboxylate)	−7.73*
					Lysine (Amino acids)	7.41*
					Serine (Amino acids)	6.73*
					4-hydroxy-3-methoxybenzoic acid (Carboxylate)	−6.23*
					Mannitol (Alcohols)	−5.89*
					Oxoproline (Amino acid derivatives)	5.89*
					Threonine (Amino acids)	5.58*
					Adenine (Others)	5.52*
					Gallic acid (Carboxylate)	5.29*
					Citric acid (Carboxylate)	5.22*
					N-acetyl-L-glutamic acid (Amino acid derivatives)	−5.06*
					Gluconic lactone (Carbohydrates)	−4.78*
					Methionine (Amino acids)	4.73*

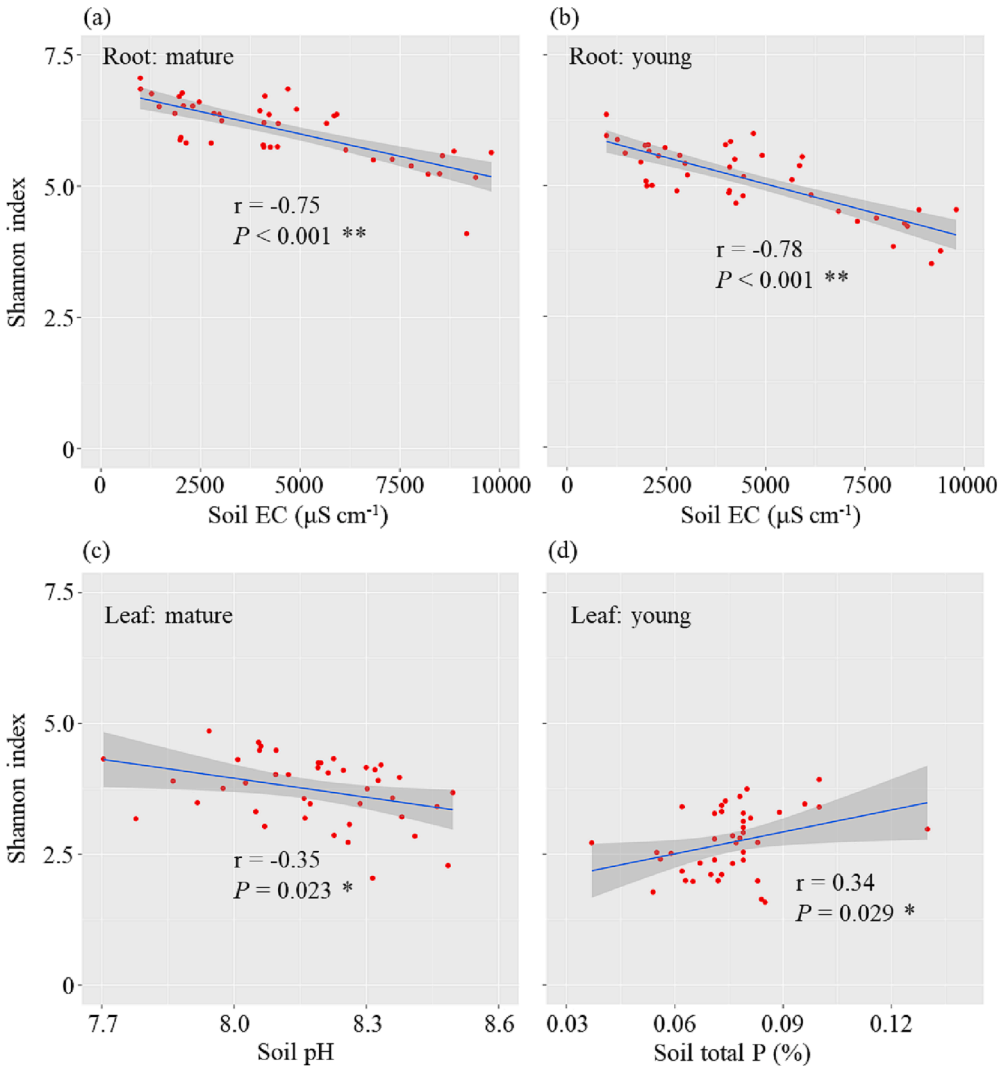

Fig. 3. The effects of edaphic factors on the diversity of endophytic communities in *Suaeda salsa* Endophytic communities include microbiome in roots and leaves of young and mature *Suaeda salsa* plants sampled from 42 sites in the Yellow River Delta, China (n = 42). For each of the plant compartments, only the significant regressions are shown. The r values are presented, and * and ** indicate significance at P < 0.05 and P < 0.01, respectively.

likely to host different microbial communities (Compant et al., 2019). Similarly, in a perennial wild mustard, *Boechera stricta*, plant organs played a greater role than plant age in determining microbiome composition and diversity (Wagner et al., 2016). Roots are embedded in soils where there is a rich diversity of bacteria, while leaves acquire microbiota mainly from the root via the xylem, and also partly from the airborne microbiome (Muller et al., 2016). This view is supported by our finding of lower microbial diversity in leaves than in roots (Fig. 1b).

Significant correlations between the microbiome composition of young and mature plants were found for both roots and leaves (Fig. S3). Plant development from vegetative to reproductive growth is accompanied by changes in metabolism in both roots and leaves that influenced the associated microbiomes, as previously observed in annual species such as *Arabidopsis* (Chaparro et al., 2014), rice (Edwards et al., 2018), and sorghum (Xu et al., 2018), while the dynamics of microbiome in perennial plants showed no response to flowering (Dombrowski et al., 2017) which is similar to our results here for *S. salsa*, a perennial species.

4.2. Soil salinity influenced the root microbiome of S. Salsa

Soil salinity played a crucial role in shaping the root microbiome structure, and salinity was negatively associated with the alpha-diversity of root-inhabiting microbiota (Table 3 and Fig. 3a and b). Increased soil salinity leads to osmotic stress, ion toxicity, and less available nutrients for both soil microbes and plants (Yan et al., 2015). Soil salinity and pH have been identified as the key drivers modulating soil microbiomes, especially in coastal sediments (Bahram et al., 2018; Delgado-Baquerizo et al., 2018; Lozupone and Knight, 2007) that have similar environmental features to the soils sampled in the present research. However, our finding implies that soil salinity didn't affect the structure and diversity of the microbiome in bulk soil, but did influence the microbiome present inside the root of the halophyte, although the root microbiome mainly originated from the soil microbial pool (Fig. 4a). Therefore, the selection force exerted by the halophyte root for soil microbes is sensitive to variations in soil salinity. In addition, plant age didn't affect the responses of root microbiomes to soil salinity gradients, possibly due to the close association between microbiome structures of young and mature roots (Fig. S3).

A dispersal effect (indicated by the effect of geographical location and soil age) on root microbiome composition or diversity was not detected in our study (Fig. 2a), possibly because the *S. salsa* plants were collected from highly saline environments (EC: 990 to 9800 μS cm^{-1}), which likely had a deterministic effect in influencing the root selectivity for the soil microbiome that was greater than any dispersal effect. In contrast, our previous study sampling *Melilotus officinalis* from the non-saline or slightly saline soils (EC: 250 to 2100 μS cm^{-1}) in the YRD

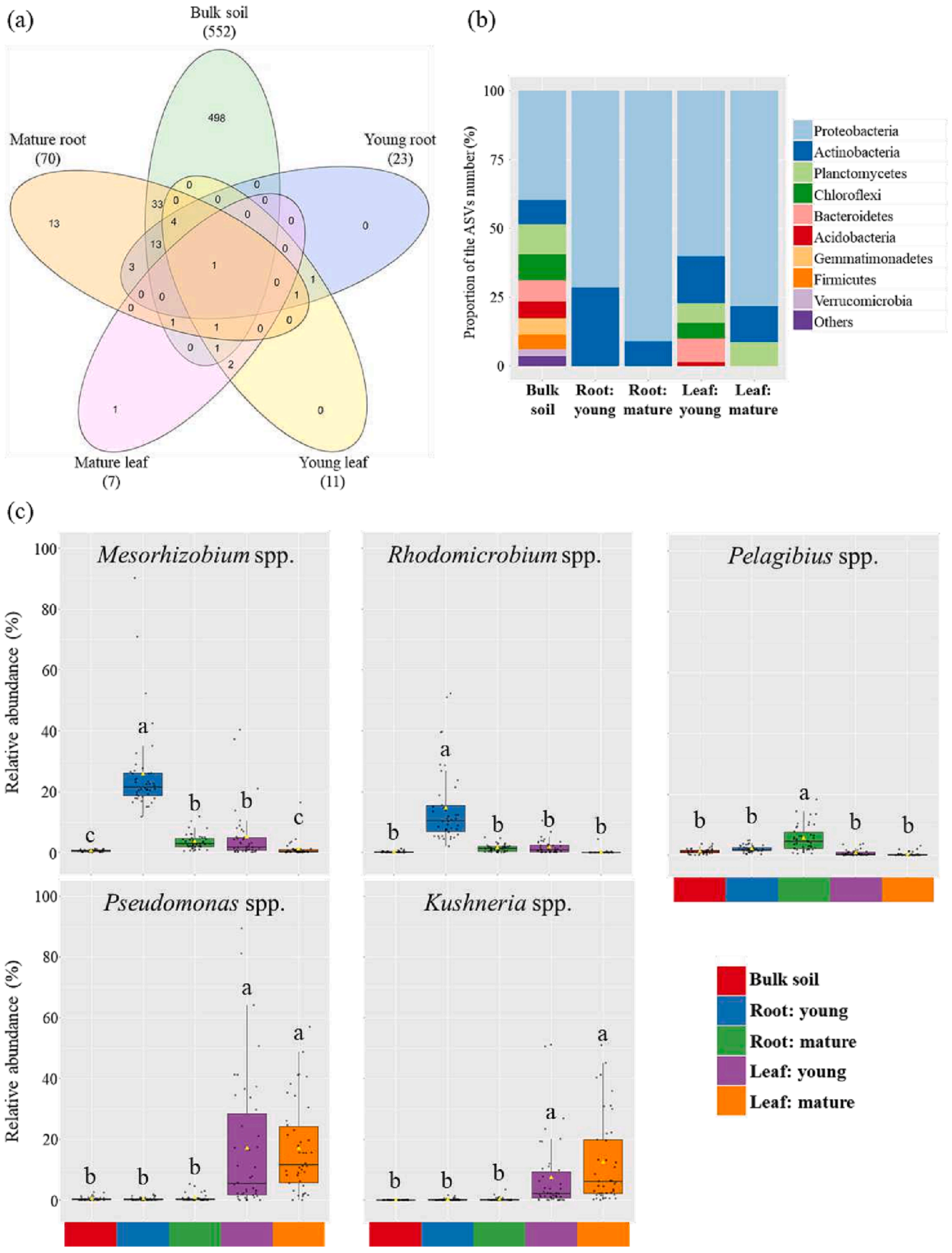

Fig. 4. Core microbiomes present in bulk soil, roots and leaves of young and mature *Suaeda salsa* plants based on samples from 42 sites in the Yellow River Delta, China. (a) Comparison of coreASVs present in five niches. coreASVs are defined as the ASVs with the top 10% mean relative abundance across all samples and present in > 80% of all samples. (b) the taxonomic annotation of coreASVs at phylum level. (c) the relative abundance of dominant bacterial genera in plant-soil niches of *Suaeda salsa*. Plant niches include roots and leaves of young and mature plants. In the boxplot, the values of individual samples are presented, the yellow triangle is the mean, and the box and central line represent first quartiles, medians, and third quartiles, respectively. The distribution of data points along the horizontal axis within each box is randomized. The same letters indicate no significant differences between niches based on the adjusted $P < 0.05$ using the Benjamini-Hochberg FDR method.

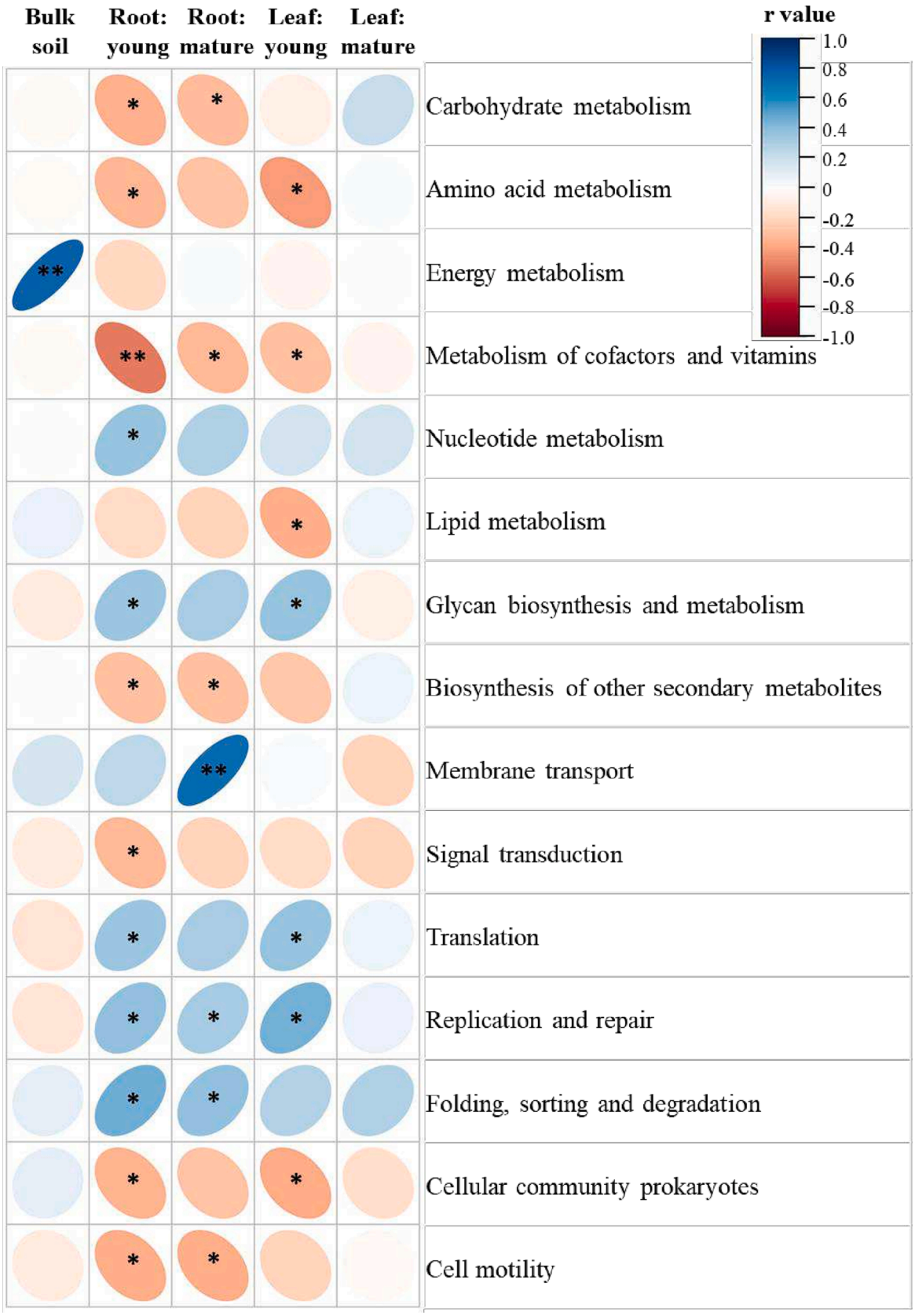

Fig. 5. Correlations between soil salinity and relative abundance of microbial functional groups in plant-soil niches of *Suaeda salsa* Plant niches include roots and leaves of young and mature *Suaeda salsa* plants sampled from 42 sites in the Yellow River Delta, China (n = 42). The P values were adjusted using the Benjamini-Hochberg FDR method. Significance levels are indicated by * and ** referring to the adjusted $P < 0.05$ and adjusted $P < 0.01$, respectively.

showed that dissimilarity of endosphere microbiomes was associated with geographic distance (Zhou et al., 2022). Therefore, the ecological process shaping the root microbiome of this halophyte under highly saline environments is different from the responses from a glycophyte or crop plants.

4.3. Dispersal effects, edaphic factors, host genetic variation and leaf metabolites influenced the structure and diversity of the S. Salsa leaf microbiome

Unlike the root microbiome, the structure and diversity of leaf microbiomes were not influenced by soil salinity, but were determined by the dispersal effects e.g., geographic distance and soil age, and the soil traits related to host plant growth (soil pH and total P). Compared with the root habitat, the leaf ecosystem is more open and fluctuating, being inherently and frequently disturbed by air movement, precipitation, UV light, and animal vectors (Muller et al., 2016), which leads to a more variable source of microbes across different locations. On the other hand, successful colonization and diversification of leaf endophytes also depends on leaf surface structure and leaf metabolites, and leaf structural and chemical heterogeneity is related to the plant genotype and species (Chaudhry et al., 2021). A study of leaf microbiomes in 56 tree species showed that there was a correlation between plant phylogeny and leaf bacterial community composition (Redford et al., 2010). Bulgarelli et al. (2013) summarised that leaf microbiome assemblies are more defined by host plant genotype, while root-associated microbiota are structured by soil properties, which is supported by our results. While we found that leaf microbiome structure of halophyte ecotypes was highly determined by the geographic effect, it was not related to their phylogenetic variation when geographic effect was controlled as a covariate (Fig S3).

In the present study, the leaf microbiome was not associated with the root microbiome (Fig. S3), with respect to composition and diversity. A strong overlap in taxonomic membership between leaf and root microbiota has been found in grapes and in *Arabidopsis* (Bai et al., 2015; Zarraonaindia et al., 2015), while for halophytes growing in hypersaline environments, the recruitment and diversification of leaf endophytes may be explained by a metabolic model in which the leaf metabolome is influenced by soil microbiomes, nutrients, and salinity stress (Badri et al., 2013; Daleo et al., 2018; Fahimipour et al., 2017). In addition, we observed a strong association between leaf microbiome diversity and the abundance of specific metabolites produced in the leaf (Table 3), which supports the metabolic model. Certain leaf metabolites that correlate with leaf microbiome structure and diversity here are also involved in plant signalling pathways that respond to salt stress, *e.g.*, tyrosine (Xin et al., 2021), or may act as precursors or substrates for the biosynthesis of key compounds with diverse functions in plant growth and adaptation to stress, *e.g.*, gluconic lactone, threitol, aspartic acid, tartaric acid, and pyridine derivatives (Burbidge et al., 2021; Cheng et al., 2022; Jia et al., 2020; Li and Song, 2019).

4.4. Core, unique and dominant microbial taxa in S. Salsa roots and leaves

Based on the microbiomes of *S. salsa* plant tissues from 42 different growing environments, we established core microbiomes and identified the dominant taxa present in roots and leaves. Interestingly, the dominant bacterial groups in *S. salsa* endophytic communities differed from those reported in studies of non-halophytic plants. The dominant taxa in the present study were *Mesorhizobium* spp. and *Rhodomicrobium* spp. in young roots, *Pelagibius* spp. in mature roots, and *Pseudomonas* spp. and *Kushneria* spp. in leaves. In the leaves of *Arabidopsis*, soybean, clover, and grapevine, the most abundant bacterial genera were *Methylobacterium* spp., *Pseudomonas* spp. and *Sphingomonas* spp. (Delmotte et al., 2009; Zarraonaindia et al., 2015). Except for *Pseudomonas* spp., the above-mentioned taxa were not detected as dominant bacteria in the core microbiomes of *S. salsa*.

Our results revealed that the enrichment of *Pelagibius* spp. and *Kushneria* spp. occurred only in mature plants. A study on Jerusalem artichoke (*Helianthus tuberosus* L.) found that *Pelagibius* spp. was more abundant in the root endophytic community when soil salinity increased (Yang et al., 2016). In addition, *Kushneria* spp. is considered as a typical halotolerant microorganism with adaptation to $>$ 1% NaCl concentration, about 10^5 μS cm^{-1} (Ventosa et al., 1998). In the *Kushneria* spp. genome, a large number of genes involved in potassium movement and osmoregulation were identified that influence salt tolerance (Yun and Bae, 2018). In another halophytic plant, *Salicornia europaea*, *Kushneria* spp. was the dominant bacterial genus in the shoot, but not in the root (Furtado et al., 2019), which is in line with our results here. *Pluchea absinthioides*, growing in the extreme environment of the Atacama Desert, Chile, (the driest nonpolar location in the world), was also highly colonised by *Kushneria* spp. in both the root and shoot (Zhang et al., 2019). In addition, we have identified a group of primary metabolites positively correlated with the relative abundance of *Kushneria* spp. in mature leaves of *S. salsa*, including fructose, D-arabitol, ornithine, naringenin and proline, which have been widely detected in *S. salsa* leaves, and were upregulated when plants were exposed to high salinity (Li and Song, 2019; Wang et al., 2019; Wu et al., 2012; Yadav et al., 2021).

4.5. Soil microbiome was only influenced by soil age

Soil age had the greatest influence on the composition and diversity of microbiota in bulk soil, but not the geographic distance or soil edaphic factors *e.g.*, salinity or pH, as reported in previous studies (Herlemann et al., 2011; Horner-Devine et al., 2004; Lozupone and Knight, 2007). The review by Hanson et al. (2012) highlighted that the distance–decay relationship could be weak or non-existent where the dispersal process becomes stronger. The YRD, where our soils were sampled, is a highly mobile system of soil formation primarily driven by sediment deposition of the Yellow River, so geographic distance and the variability of typical soil salinity processes appear to be of lesser influence. The Yellow River, has the highest sediment load in the world, and almost half of the transported sediment is deposited in the YRD, with frequent channel migrations, which form about 9 km^2 new land every year (Gao et al., 2018; Guan et al., 2019). Previous studies confirm that soil chronosequence can drive the diversity of soil microbiomes over time frames encompassing thousands to millions of years (Delgado-Baquerizo et al., 2019; Teste et al., 2021). Our soils were collected from young land, with the age differences of only 60–120 years, and the association between soil age and microbiome diversity suggests that the dispersal history of sediment deposition from the river is a key driver determining the soil microbiome assembly.

4.6. Predicted functions of microbiome in S. Salsa roots and leaves

The predicted function profiles of microbiomes in the studied niches imply that carbohydrate metabolism and signal transduction activities were highly abundant in the leaf microbiota, possibly because *S. salsa* is a euhalophytic herb with succulent leaves rich in carbohydrate to dilute the salt (Song and Wang, 2015). This would also provide diverse carbon sources for metabolism by leaf endophytes. Enriched signal transduction pathways could improve the microbes' ability to sense and respond to environmental change (Lajoie et al., 2020), and the ability to adapt to the special microhabitat of succulent leaves.

Microbiota in the root had a high level of membrane transport functions, possibly because root-associated bacteria avoid the high salt concentrations via specific membrane functions that aid in maintaining cell wall structure, and/or via transporters exporting ions from the cell (Ruppel et al., 2013). The salt avoidance strategy of microbes is also supported by our finding that the relative abundance of membrane transport functions was highly associated with soil salinity for the endophytes in mature roots (Fig. 5). In addition, the root microbiomes

were highly enriched in functions related to genetic information processing, to a greater extent than carbohydrate and amino acid metabolism functions, especially for the younger plants (Fig. S7). This indicates that r-strategy bacteria may be promoted in roots by investing the available resources into reproduction, to rapidly adapt to the change in microhabitat from soil to root (Song et al., 2017).

5. Conclusions

By analysing 210 samples of soils and *S. salsa* roots and leaves from 42 different growing environments in the Yellow River Delta, we identified that there was a strong deterministic process of soil salinity on the diversity and composition of the endophyte community in roots but not leaves, and core microbes of *S. salsa* included *Rhodomicrobium* spp., *Pelagibius* spp., and *Kushneria* spp. which were not detected in other non-halophytes before. Our finding provides an important cue for understanding the mechanisms for salt tolerance of halophytes in the aspect of the hologenome.

Declaration of Competing Interest

The authors declare that they have no known competing financial interests or personal relationships that could have appeared to influence the work reported in this paper.

Data availability

Data will be made available on request.

Acknowledgements

We thank the staff from the Yellow River Delta National Forest Park for assistance with the plant and soil collection.

Funding

This work was supported by the Australian Research Council (IH140100013 and LP200200813), the Grains Research and Development Corporation, the Department of Trade, Tourism and Investment of the South Australian Government, Shandong Provincial Natural Science Foundation (project ID: ZR2019BC076), and the University of Adelaide.

Appendix A. Supplementary data

Supplementary data to this article can be found online at https://doi.org/10.1016/j.geoderma.2023.116447.

References

Afendi, F.M., Okada, T., Yamazaki, M., Hirai-Morita, A., Nakamura, Y., Nakamura, K., Ikeda, S., Takahashi, H., Altaf-Ul-Amin, M., Darusman, L.K., 2012. KNApSAcK family databases: integrated metabolite–plant species databases for multifaceted plant research. Plant Cell Physiol. 53, e1–e.

Aßhauer, K.P., Wemheuer, B., Daniel, R., Meinicke, P., 2015. Tax4Fun: predicting functional profiles from metagenomic 16S rRNA data. Bioinformatics 31, 2882–2884.

Badri, D.V., Zolla, G., Bakker, M.G., Manter, D.K., Vivanco, J.M., 2013. Potential impact of soil microbiomes on the leaf metabolome and on herbivore feeding behavior. New Phytol. 198, 264–273.

Bahram, M., Hildebrand, F., Forslund, S.K., Anderson, J.L., Soudzilovskaia, N.A., Bodegom, P.M., Bengtsson-Palme, J., Anslan, S., Coelho, L.P., Harend, H., Huerta-Cepas, J., Medema, M.H., Maltz, M.R., Mundra, S., Olsson, P.A., Pent, M., Polme, S., Sunagawa, S., Ryberg, M., Tedersoo, L., Bork, P., 2018. Structure and function of the global topsoil microbiome. Nature 560, 233–237.

Bai, Y., Mueller, D.B., Srinivas, G., Garrido-Oter, R., Potthoff, E., Rott, M., Dombrowski, N., Muench, P.C., Spaepen, S., Remus-Emsermann, M., Huettel, B., McHardy, A.C., Vorholt, J.A., Schulze-Lefert, P., 2015. Functional overlap of the *Arabidopsis* leaf and root microbiota. Nature 528, 364–369.

Bolyen, E., Rideout, J.R., Dillon, M.R., Bokulich, N.A., Abnet, C.C., Al-Ghalith, G.A., Alexander, H., Alm, E.J., Arumugam, M., Asnicar, F., 2019. Reproducible, interactive, scalable and extensible microbiome data science using QIIME 2. Nat. Biotechnol. 37, 852–857.

Bulgarelli, D., Rott, M., Schlaeppi, K., van Themaat, E.V.L., Ahmadinejad, N., Assenza, F., Rauf, P., Huettel, B., Reinhardt, R., Schmelzer, E., Peplies, J., Gloeckner, F.O., Amann, R., Eickhorst, T., Schulze-Lefert, P., 2012. Revealing structure and assembly cues for *Arabidopsis* root-inhabiting bacterial microbiota. Nature 488, 91–95.

Bulgarelli, D., Schlaeppi, K., Spaepen, S., van Themaat, E.V.L., Schulze-Lefert, P., 2013. Structure and functions of the bacterial microbiota of plants. Annu. Rev. Plant Biol. 64, 807–838.

Burbidge, C.A., Ford, C.M., Melino, V.J., Wong, D.C.J., Jia, Y., Jenkins, C.L.D., Soole, K. L., Castellarin, S.D., Darriet, P., Rienth, M., 2021. Biosynthesis and cellular functions of tartaric acid in grapevines. Front. Plant Sci. 12, 309.

Callahan, B.J., McMurdie, P.J., Rosen, M.J., Han, A.W., Johnson, A.J.A., Holmes, S.P., 2016. DADA2: high-resolution sample inference from Illumina amplicon data. Nat. Methods 13, 581–583.

Castresana, J., 2000. Selection of conserved blocks from multiple alignments for their use in phylogenetic analysis. Mol. Biol. Evol. 17, 540–552.

Cernava, T., Erlacher, A., Soh, J., Sensen, C.W., Grube, M., Berg, G., 2019. Enterobacteriaceae dominate the core microbiome and contribute to the resistome of arugula (*Eruca sativa* Mill.). Microbiome 7.

Chaparro, J.M., Badri, D.V., Vivanco, J.M., 2014. Rhizosphere microbiome assemblage is affected by plant development. ISME J. 8, 790–803.

Chaudhry, V., Runge, P., Sengupta, P., Doehlemann, G., Parker, J.E., Kemen, E., 2021. Shaping the leaf microbiota: plant–microbe–microbe interactions. J. Exp. Bot. 72, 36–56.

Cheng, B., Hassan, M.J., Feng, G., Zhao, J., Liu, W., Peng, Y., Li, Z., 2022. Metabolites reprogramming and Na+/K+ transportation associated with putrescine-regulated white clover seed germination and seedling tolerance to salt toxicity. Front. Plant Sci. 13.

Cohen, H., Matityahu, I., Amir, R., 2016. Metabolite Profiling of Mature Arabidopsis thaliana Seeds Using Gas Chromatography-Mass Spectrometry (GC-MS). Bio-protocol 6, e1981.

Compant, S., Samad, A., Faist, H., Sessitsch, A., 2019. A review on the plant microbiome: Ecology, functions, and emerging trends in microbial application. J. Adv. Res. 19, 29–37.

Daleo, P., Alberti, J., Jumpponen, A., Veach, A., Ialonardi, F., Iribarne, O., Silliman, B., 2018. Nitrogen enrichment suppresses other environmental drivers and homogenizes salt marsh leaf microbiome. Ecology 99, 1411–1418.

Delgado-Baquerizo, M., Oliverio, A.M., Brewer, T.E., Benavent-González, A., Eldridge, D. J., Bardgett, R.D., Maestre, F.T., Singh, B.K., Fierer, N., 2018. A global atlas of the dominant bacteria found in soil. Science 359, 320–325.

Delgado-Baquerizo, M., Bardgett, R.D., Vitousek, P.M., Maestre, F.T., Williams, M.A., Eldridge, D.J., Lambers, H., Neuhauser, S., Gallardo, A., Garcia-Velazquez, L., Sala, O.E., Abades, S.R., Alfaro, F.D., Berhe, A.A., Bowker, M.A., Currier, C.M., Cutler, N.A., Hart, S.C., Hayes, P.E., Hseu, Z.Y., Kirchmair, M., Pena-Ramirez, V.M., Perez, C.A., Reed, S.C., Santos, F., Siebe, C., Sullivan, B.W., Weber-Grullon, L., Fierer, N., 2019. Changes in belowground biodiversity during ecosystem development. Proc. Natl. Acad. Sci. U.S.A. 116, 6891–6896.

Delmotte, N., Knief, C., Chaffron, S., Innerebner, G., Roschitzki, B., Schlapbach, R., von Mering, C., Vorholt, J.A., 2009. Community proteogenomics reveals insights into the physiology of phyllosphere bacteria. Proc. Natl. Acad. Sci. U.S.A. 106, 16428–16433.

Dombrowski, N., Schlaeppi, K., Agler, M.T., Hacquard, S., Kemen, E., Garrido-Oter, R., Wunder, J., Coupland, G., Schulze-Lefert, P., 2017. Root microbiota dynamics of perennial Arabis alpina are dependent on soil residence time but independent of flowering time. ISME J. 11, 43–55.

Doyle, J.J., Doyle, J.L., 1990. Isolation of DNA from fresh tissue. Focus 12, 13–15.

Edwards, J.A., Santos-Medellín, C.M., Liechty, Z.S., Nguyen, B., Lurie, E., Eason, S., Phillips, G., Sundaresan, V., 2018. Compositional shifts in root-associated bacterial and archaeal microbiota track the plant life cycle in field-grown rice. PLOS Biol. 16, e2003862.

Fahimipour, A.K., Kardish, M.R., Lang, J.M., Green, J.L., Eisen, J.A., Stachowicz, J.J., 2017. Global-scale structure of the eelgrass microbiome. Appl. Environ, Microbiol, p. 83.

Furtado, B.U., Golebiewski, M., Skorupa, M., Hulisz, P., Hrynkiewicz, K., 2019. Bacterial and fungal endophytic microbiomes of *Salicornia europaea*. Appl. Environ, Microbiol, p. 85.

Gao, P., Wang, Y., Li, P., Zhao, G., Sun, W., Mu, X., 2018. Land degradation changes in the Yellow River Delta and its response to the streamflow-sediment fluxes since 1976. Land Degrad. Dev. 29, 3212–3220.

Grady, K.L., Sorensen, J.W., Stopnisek, N., Guittar, J., Shade, A., 2019. Assembly and seasonality of core phyllosphere microbiota on perennial biofuel crops. Nat, Commun, p. 10.

Guan, B., Chen, M., Elsey-Quirk, T., Yang, S., Shang, W., Li, Y., Tian, X., Han, G., 2019. Soil seed bank and vegetation differences following channel diversion in the Yellow River Delta. Sci. Total Environ. 693, 133600.

Guan, Y., Jiang, N., Wu, Y., Yang, Z., Bello, A., Yang, W., 2021. Disentangling the role of salinity-sodicity in shaping soil microbiome along a natural saline-sodic gradient. Sci. Total Environ. 765, 142738.

Hanson, C.A., Fuhrman, J.A., Horner-Devine, M.C., Martiny, J.B., 2012. Beyond biogeographic patterns: processes shaping the microbial landscape. Nat. Rev. Microbiol. 10, 497–506.

Hardoim, P.R., van Overbeek, L.S., Berg, G., Pirttilä, A.M., Compant, S., Campisano, A., Döring, M., Sessitsch, A., 2015. The Hidden world within plants: Ecological and evolutionary considerations for defining functioning of microbial endophytes. Microbiol. Mol. Biol. Rev. 79, 293–320.

Herlemann, D.P., Labrenz, M., Jürgens, K., Bertilsson, S., Waniek, J.J., Andersson, A.F., 2011. Transitions in bacterial communities along the 2000 km salinity gradient of the Baltic Sea. ISME J. 5, 1571–1579.
Horai, H., Arita, M., Kanaya, S., Nihei, Y., Ikeda, T., Suwa, K., Ojima, Y., Tanaka, K., Tanaka, S., Aoshima, K., 2010. MassBank: a public repository for sharing mass spectral data for life sciences. J. Mass Spectrom. 45, 703–714.
Horner-Devine, M.C., Lage, M., Hughes, J.B., Bohannan, B.J., 2004. A taxa–area relationship for bacteria. Nature 432, 750–753.
Jia, H., Wang, L., Li, J., Sun, P., Lu, M., Hu, J., 2020. Physiological and metabolic responses of *Salix sinopurpurea* and *Salix suchowensis* to drought stress. Trees 34, 563–577.
Jiao, S., Xu, Y., Zhang, J., Hao, X., Lu, Y., 2019. Core microbiota in agricultural soils and their potential associations with nutrient cycling. mSystems 4, e00313-00318.
Kanehisa, M., Goto, S., 2000. KEGG: kyoto encyclopedia of genes and genomes. Nucleic Acids Res. 28, 27–30.
Katoh, K., Rozewicki, J., Yamada, K.D., 2017. MAFFT online service: multiple sequence alignment, interactive sequence choice and visualization. Brief. Bioinformatics 20, 1160–1166.
Kearl, J., McNary, C., Lowman, J.S., Mei, C.S., Aanderud, Z.T., Smith, S.T., West, J., Colton, E., Hamson, M., Nielsen, B.L., 2019. Salt-tolerant halophyte rhizosphere bacteria stimulate growth of Alfalfa in salty soil. Front, Microbiol, p. 10.
Kembel, S.W., O'Connor, T.K., Arnold, H.K., Hubbell, S.P., Wright, S.J., Green, J.L., 2014. Relationships between phyllosphere bacterial communities and plant functional traits in a neotropical forest. Proc. Natl. Acad. Sci. U.S.A. 111, 13715–13720.
Lajoie, G., Maglione, R., Kembel, S.W., 2020. Adaptive matching between phyllosphere bacteria and their tree hosts in a neotropical forest. Microbiome 8, 1–10.
Li, H., La, S.K., Zhang, X., Gao, L.H., Tian, Y.Q., 2021. Salt-induced recruitment of specific root-associated bacterial consortium capable of enhancing plant adaptability to salt stress. ISME J. 15, 2865–2882.
Li, Q., Song, J., 2019. Analysis of widely targeted metabolites of the euhalophyte *Suaeda salsa* under saline conditions provides new insights into salt tolerance and nutritional value in halophytic species. BMC Plant Biol. 19, 388.
Liu, L., Huang, X., Zhang, J., Cai, Z., Jiang, K., Chang, Y., 2020b. Deciphering the relative importance of soil and plant traits on the development of rhizosphere microbial communities. Soil Biol. Biochem. 148, 107909.
Liu, F., Mo, X., Kong, W., Song, Y., 2020a. Soil bacterial diversity, structure, and function of *Suaeda salsa* in rhizosphere and non-rhizosphere soils in various habitats in the Yellow River Delta. China. Sci. Total Environ. 740, 140144.
Lozupone, C.A., Knight, R., 2007. Global patterns in bacterial diversity. Proc. Natl. Acad. Sci. U.S.A. 104, 11436–11440.
Lu, X., Chen, Q., Cui, X., Abozeid, A., Liu, Y., Liu, J., Tang, Z., 2019. Comparative metabolomics of two saline-alkali tolerant plants Suaeda glauca and Puccinellia tenuiflora based on GC-MS platform. Nat. Prod. Res. 1–4.
Mallick, H., Rahnavard, A., McIver, L.J., Ma, S., Zhang, Y., Nguyen, L.H., Tickle, T.L., Weingart, G., Ren, B., Schwager, E.H., 2021. Multivariable association discovery in population-scale meta-omics studies. PLoS Comput. Biol. 17, e1009442.
Marasco, R., Mosqueira, M.J., Fusi, M., Ramond, J.B., Merlino, G., Booth, J.M., Maggs-Kolling, G., Cowan, D.A., Daffonchio, D., 2018. Rhizosheath microbial community assembly of sympatric desert speargrasses is independent of the plant host. Microbiome 6.
Massoni, J., Bortfeld-Miller, M., Jardillier, L., Salazar, G., Sunagawa, S., Vorholt, J.A., 2020. Consistent host and organ occupancy of phyllosphere bacteria in a community of wild herbaceous plant species. ISME J. 14, 245–258.
Mukhtar, S., Mehnaz, S., Malik, K.A., 2021. Comparative study of the rhizosphere and root endosphere microbiomes of Cholistan Desert plants. Front, Microbiol, p. 12.
Muller, D.B., Vogel, C., Bai, Y., Vorholt, J.A., 2016. The plant microbiota: Systems-level insights and perspectives. Annu. Rev. Genet. 50, 211–234.
Munns, R., 2005. Genes and salt tolerance: bringing them together. New Phytol. 167, 645–663.
Naylor, D., DeGraaf, S., Purdom, E., Coleman-Derr, D., 2017. Drought and host selection influence bacterial community dynamics in the grass root microbiome. ISME J. 11, 2691–2704.
Oksanen, J., Kindt, R., Legendre, P., O'Hara, B., Stevens, M.H.H., Oksanen, M.J., Suggests, M., 2007. The vegan package. Community ecology package 10, 631–637.
Park, J.-S., Takayama, K., Suyama, Y., Choi, B.-H., 2019. Distinct phylogeographic structure of the halophyte Suaeda malacosperma (Chenopodiaceae/ Amaranthaceae), endemic to Korea-Japan region, influenced by historical range shift dynamics. Plant Syst. Evol. 305, 193–203.
Parks, D.H., Tyson, G.W., Hugenholtz, P., Beiko, R.G., 2014. STAMP: statistical analysis of taxonomic and functional profiles. Bioinformatics 30, 3123–3124.
Quast, C., Pruesse, E., Yilmaz, P., Gerken, J., Schweer, T., Yarza, P., Peplies, J., Glockner, F.O., 2013. The SILVA ribosomal RNA gene database project: improved data processing and web-based tools. Nucleic Acids Res. 41, D590-D596.
R Core Team, 2013. R: A language and environment for statistical computing.
Rath, K.M., Murphy, D.N., Rousk, J., 2019. The microbial community size, structure, and process rates along natural gradients of soil salinity. Soil Biol. Biochem. 138.
Rayment, G.E., Lyons, D.J., 2011. Soil chemical methods: Australasia. CSIRO publishing.
Redford, A.J., Bowers, R.M., Knight, R., Linhart, Y., Fierer, N., 2010. The ecology of the phyllosphere: geographic and phylogenetic variability in the distribution of bacteria on tree leaves. Environ. Microbiol. 12, 2885–2893.
Ruppel, S., Franken, P., Witzel, K., 2013. Properties of the halophyte microbiome and their implications for plant salt tolerance. Funct. Plant Biol. 40, 940–951.
Saghafi, D., Delangiz, N., Lajayer, B.A., Ghorbanpour, M., 2019. An overview on improvement of crop productivity in saline soils by halotolerant and halophilic PGPRs. 3 Biotech 9.
Shaw, J., Lickey, E.B., Schilling, E.E., Small, R.L., 2007. Comparison of whole chloroplast genome sequences to choose noncoding regions for phylogenetic studies in angiosperms: the tortoise and the hare III. Am. J. Bot. 94, 275–288.
Silvestro, D., Michalak, I., 2012. raxmlGUI: a graphical front-end for RAxML. Org. Divers. Evol. 12, 335–337.
Song, H.-K., Song, W., Kim, M., Tripathi, B.M., Kim, H., Jablonski, P., Adams, J.M., 2017. Bacterial strategies along nutrient and time gradients, revealed by metagenomic analysis of laboratory microcosms. FEMS Microbiol, Ecol, p. 93.
Song, J., Wang, B., 2015. Using euhalophytes to understand salt tolerance and to develop saline agriculture: Suaeda salsa as a promising model. Ann. Bot. 115, 541–553.
Sun, A.Q., Jiao, X.Y., Chen, Q.L., Wu, A.L., Zheng, Y., Lin, Y.X., He, J.Z., Hu, H.W., 2021. Microbial communities in crop phyllosphere and root endosphere are more resistant than soil microbiota to fertilization. Soil Biol. Biochem. 153.
Szymanska, S., Borruso, L., Brusetti, L., Hulisz, P., Furtado, B., Hrynkiewicz, K., 2018. Bacterial microbiome of root-associated endophytes of Salicornia europaea in correspondence to different levels of salinity. Environ. Sci. Pollut. Res. 25, 25420–25431.
Teste, F.P., Lambers, H., Enowashu, E.E., Laliberte, E., Marhan, S., Kandeler, E., 2021. Soil microbial communities are driven by the declining availability of cations and phosphorus during ecosystem retrogression. Soil Biol. Biochem. 163.
Thijs, S., Op De Beeck, M., Beckers, B., Truyens, S., Stevens, V., Van Hamme, J.D., Weyens, N., Vangronsveld, J., 2017. Comparative evaluation of four bacteria-specific primer pairs for 16S rRNA gene surveys. Front. Microbiol. 8, 494.
Ventosa, A., Nieto, J.J., Oren, A., 1998. Biology of moderately halophilic aerobic bacteria. Microbiol. Mol. Biol. Rev. 62, 504–544.
Vimal, S.R., Singh, J.S., Arora, N.K., Singh, S., 2017. Soil-plant-microbe interactions in stressed agriculture management: a review. Pedosphere 27, 177–192.
Wagner, M.R., Lundberg, D.S., del Rio, T.G., Tringe, S.G., Dangl, J.L., Mitchell-Olds, T., 2016. Host genotype and age shape the leaf and root microbiomes of a wild perennial plant. Nat, Commun, p. 7.
Wang, X., Bai, J.H., Wang, W., Zhang, G.L., 2019. Leaf metabolites profiling between red and green phenotypes of *Suaeda salsa* by widely targeted metabolomics. Funct. Plant Biol. 46, 845–856.
Wang, Y., Xu, L., Shen, H., Wang, J., Liu, W., Zhu, X., Wang, R., Sun, X., Liu, L., 2015. Metabolomic analysis with GC-MS to reveal potential metabolites and biological pathways involved in Pb & Cd stress response of radish roots. Sci. Rep. 5, 18296.
Wu, H.F., Liu, X.L., You, L.P., Zhang, L.B., Zhou, D., Feng, J.H., Zhao, J.M., Yu, J.B., 2012. Effects of salinity on metabolic profiles, gene expressions, and antioxidant enzymes in halophyte *Suaeda salsa*. J. Plant Growth Regul. 31, 332–341.
Xin, J., Li, C., Ning, K., Qin, Y., Shang, J.X., Sun, Y., 2021. AtPFA-DSP3, an atypical dual-specificity protein tyrosine phosphatase, affects salt stress response by modulating MPK3 and MPK6 activity. Plant Cell Environ. 44, 1534–1548.
Xu, L., Naylor, D., Dong, Z., Simmons, T., Pierroz, G., Hixson, K.K., Kim, Y.-M., Zink, E. M., Engbrecht, K.M., Wang, Y., 2018. Drought delays development of the sorghum root microbiome and enriches for monoderm bacteria. Proc. Natl. Acad. Sci. U.S.A. 115, E4284-E4293.
Yadav, S., Elansary, H.O., Mattar, M.A., Elhindi, K.M., Alotaibi, M.A., Mishra, A., 2021. Differential accumulation of metabolites in *Suaeda* species provides new insights into abiotic stress tolerance in C-4-halophytic species in elevated CO2 conditions. Agronomy-Basel 11.
Yan, N., Marschner, P., Cao, W., Zuo, C., Qin, W., 2015. Influence of salinity and water content on soil microorganisms. Int. Soil Water Conserv. Res. 3, 316–323.
Yang, H., Hu, J., Long, X., Liu, Z., Rengel, Z., 2016. Salinity altered root distribution and increased diversity of bacterial communities in the rhizosphere soil of Jerusalem artichoke. Sci. Rep. 6, 1–10.
Yuan, Z., Druzhinina, I.S., Labbe, J., Redman, R., Qin, Y., Rodriguez, R., Zhang, C., Tuskan, G.A., Lin, F., 2016. Specialized microbiome of a halophyte and its role in helping non-host plants to withstand salinity. Sci, Rep, p. 6.
Yun, J.-H., Bae, J.-W., 2018. Complete genome sequence of the halophile bacterium Kushneria marisflavi KCCM 80003T, isolated from seawater in Korea. Mar. Genomics 37, 35–38.
Zang, W., Miao, R.Q., Zhang, Y., Yuan, Y., Pang, Q.Y., Zhou, Z.Q., 2021. Metabolic and molecular basis for the salt and alkali responses of Suaeda corniculata. Environ. Exp, Bot, p. 192.
Zarraonaindia, I., Owens, S.M., Weisenhorn, P., West, K., Hampton-Marcell, J., Lax, S., Bokulich, N.A., Mills, D.A., Martin, G., Taghavi, S., van der Lelie, D., Gilbert, J.A., 2015. The soil microbiome influences grapevine-associated microbiota. Mbio 6.
Zhang, Q., Acuna, J.J., Inostroza, N.G., Mora, M.L., Radic, S., Sadowsky, M.J., Jorquera, M.A., 2019. Endophytic bacterial communities associated with roots and leaves of plants growing in Chilean extreme environments. Sci, Rep, p. 9.
Zhao, Y.H., Li, T., Shao, P.S., Sun, J.K., Xu, W.J., Zhang, Z.H., 2022. Variation in bacterial community structure in rhizosphere and bulk soils of different halophytes in the Yellow River Delta. Front. Ecol, Evol, p. 9.
Zhou, Y., Coventry, D.R., Gupta, V.V., Fuentes, D., Merchant, A., Kaiser, B.N., Li, J., Wei, Y., Liu, H., Wang, Y., 2020. The preceding root system drives the composition and function of the rhizosphere microbiome. Genome Biol. 21, 1–19.
Zhou, Y., Wei, Y., Zhao, Z., Li, J., Li, H., Yang, P., Tian, S., Ryder, M., Toh, R., Yang, H., 2022. Microbial communities along the soil-root continuum are determined by root anatomical boundaries, soil properties, and root exudation. Soil Biol. Biochem. 108721.